Instrumented Piles Tested in 1969 in Fine Loose Sand at Holmen, Drammen: Revisited 2019

A.S. Balasubramaniam[1], J.M.N.S. Jayasiri[2], E. Oh[3], G. Chao[2], H. Kim[4], R. N. Hwang[5]

[1,3]*School of Engineering, Griffith University, Gold Coast, Australia*
[2]*Asian Institute of Technology, Bangkok, Thailand*
[4]*AICLOPS, Goyang-si, Republic of Korea*
[5]*Moh and Associates, New Taipei City, Taiwan, Republic of China*
E-mail: bala.b.balasubramaniam@griffith.edu.au

ABSTRACT: The work presented here relates to the instrumented piles tested in 1969, by the Norwegian Geotechnical Institute (NGI) in loose sand at Holmen, Drammen. The material contained in the first publication, which is an Internal Report F.273.0 of NGI (Balasubramaniam et al., 1969), was mainly on the load tests only and contained the analyses of the vibrating wire gauges as based on the zero of the gauges after the pile driving, to make sure the best set of zero values were used. The publication of Gregersen et al. in 1969, includes pull out tests and also the effect of the residual stresses developed in the piles during pile driving. Further, the work of Gregersen et al. contains a detail section on the performance of the vibrating wire gauges and in particular the drifting of the zero of the gauges. The entire pile testing work and reporting in NGI internal report F.273.0 (Balasubramaniam et al., 1969) included a description of the instrumentation used and the results obtained from load and pull out tests on precast reinforced concrete piles. The piles, of circular cross section and available in standard lengths, can be joined together in the field by means of threaded connectors. The primary purpose of the instrumentation was to determine the distribution of axial load along the length of the pile and the point load and also to measure the distribution of lateral earth pressure acting on the periphery of the pile. To accomplish these goals, the piles were equipped at a number of levels with strain gauges embedded in the concrete, on the reinforcing steel, and earth pressure cells on the sides of the piles, together with hydraulic piezometers for measuring pore water pressure in the sand. The instrumentation system was based on the operating principle of the vibrating-wire strain gauge (Bjerrum et al., 1965). Altogether four instrumented piles were used in the test program, three cylindrical and the fourth conical in shape, and had a uniform taper, typical for a Norwegian timber pile. The piles were constructed in such a manner that the 8m long cylindrical and conical piles can be tested first and later, after completion of these tests each one of them can be lengthened by connecting additional 8m segment of instrumented cylindrical pile to make up two 16 m long test piles. The test program also included additional tests on a single pile, which was made up of 4 m long precast concrete pile sections driven one section at a time and tested for embedded lengths of 3.5, 7.5, 11.5, 15.5, 19.5 and 23.5 m; the latter pile only had load cell at the top to measure the applied load and was not instrumented.

KEYWORDS: Pile load test, Bearing capacity, Pull out test

1. INTRODUCTION

On the recommendation of late Prof. Kenneth Harry Roscoe, late Dr Laurits Bjerrum took me, the first author, as a post-doctoral fellow at NGI in 1969. All my previous work was on laboratory triaxial tests at Cambridge University. NGI had an excellent laboratory. I was new to field tests and instrumentation. I was fortunate to work under Dr Elmo DiBiagio, the head of the instrumentation group. Dr DiBiagio was very polite and educated me a lot. One of the most popular projects I worked under Dr DiBiagio was the instrumented piles tested at Holmen Drammen in loose sand. It was an interesting time at NGI where the vibrating wire instruments; strain gauges in steel, concrete, earth pressure cells and inclinometers were tested continuously for their reliability and application. One of the problems investigated was the drifting of the zero of the strain gauges with time.

The pile testing program offered a unique opportunity to study the performance of vibrating wire gauge instruments, when subjected to pile driving, loading and also pulling out when tensile stresses develop in the concrete and the piles crack. In this project several instruments were used. Load cells were used to measure the point load at the tip of the pile, and the piles were equipped at a number of levels with strain gauges embedded in the concrete, strain gauges on the reinforcing steel, and earth pressure cells on the sides of the piles, together with hydraulic piezometers for measuring pore water pressure in the sand. The instrumentation system was based on the operating principle of the vibrating-wire strain gauge (Bjerrum et al., 1965).

The main purpose of the instrumentation was to determine the distribution of axial load along the length of the pile and the point load, and additionally to check the performance of the earth pressure cells. Axial loads were measured at seven cross sections along the length of the pile. At each of these sections a single embedment vibrating-wire deformation gauge was installed as close as possible to the centre of the pile in order to measure strains in the concrete. Similarly, a vibrating-wire strain gauge was attached to the surface of each of the four reinforcing steel bars. The gauges on the reinforcing steel were symmetrically placed on two orthogonal diameters in the cross section. By taking the average of the four strain gauge readings the effects of any bending stresses in the pile could be eliminated.
The topics covered in this paper include;

1) The site conditions at Holmen Drammen: Four static cone penetration tests (CPTs), one standard penetration test (SPT) and one sample boring were carried out at the test site prior to the pile loading tests. The natural density, water content and the grain size distribution of the sand were determined.
2) A detail understanding of the pile driving and the usefulness in establishing the homogeneity of the sand deposit was made by the number of blows needed to drive the test piles and the anchor piles.
3) A full description of the instruments used and their calibration: this includes the load cell used at the base of the piles, the earth pressure cells used in the piles, and gauges developed to measure stresses and strains in concrete and the reinforcement steel;
4) The full testing program of load tests and pull out tests.
5) A complete analysis of the results to understand the residual stresses in the piles as carried out by Gregersen et al. (1973) after pile driving and their effect during load tests; load-settlement diagram as obtained from the pile testing; distribution of axial loads in the piles; skin friction values estimated in the piles; estimation of the bearing capacity Q_{90}. Q_{90} is defined as the load at which the settlement is twice as large as the settlement at 90% of the load from load-settlement curves (Fellenius, 1975); and a detail presentation and interpretation of the data from the earth pressure measurements.

2. TEST CONDITIONS

2.1 Site Conditions

A description of the site conditions has already been given in Gregersen, et al. (1973). The test site shown in Figure 1 is located on a small island called Holmen in the middle of the Drammen river near the city of Drammen. The soil profile consists of a 1-m thick surface layer of sandy fill containing some gravels which is underlain by a stratum of fine to medium grained sand down to a depth of 3 m. Below a depth of 3 m and down to about 30 m there is a deposit of medium to coarse grained sand. The natural ground water table is about 1.7 m below the surface. The point resistance values obtained from CPT test indicate that the top 5 m of the profile consists of well compacted sand for which the point resistance increases linearly to a maximum value of about 7.5 MPa at a depth of 4 m. Further, at a depth of 5 m, there is a sudden drop in penetration resistance to approximately 2.5 MPa followed by a more or less linear increase in the point resistance with depth down to the end of the boring.

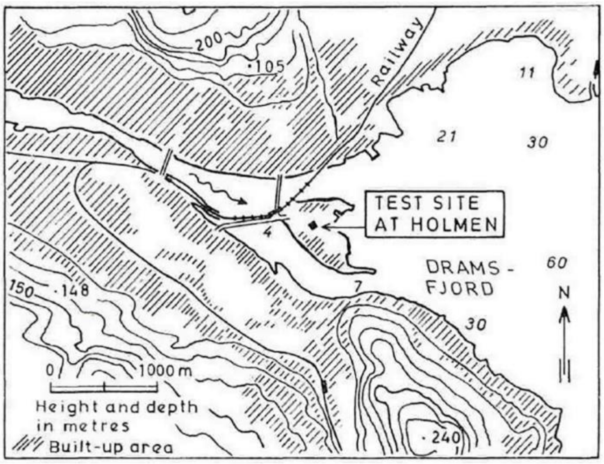

Figure 1 Test site location in Holman, Drammen
(after Gregersen et al 1973)

Four CPTs, one SPT and one sample boring were carried out at the test site prior to the pile loading tests. Typical results from the tests are shown in Figure 2. Since the sampling technique used to obtain samples probably caused some compaction of the sand, the density values determined from the laboratory investigations might not be exactly representative of the in situ conditions. For this reason, the interpretation of this data should be guided by the results of the CPT which gave consistent and reliable values at this site.

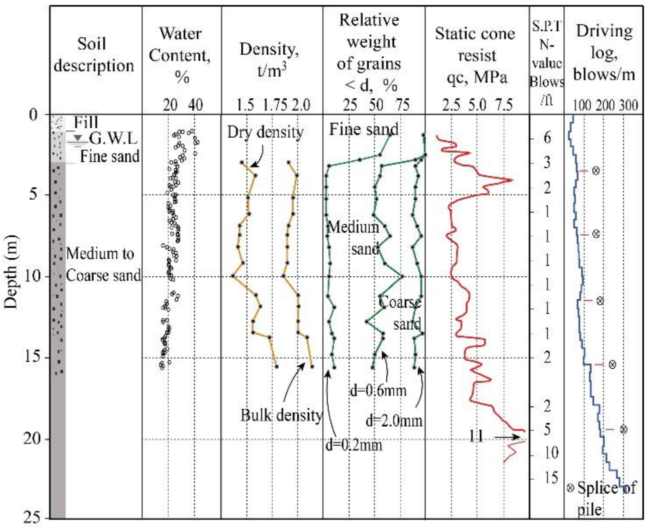

Figure 2 Soil profile at Holmen Drammen

Since both SPT and CPT tests are commonly used for predicting the bearing capacity of piles, empirical relationships have been developed to relate the SPT N-value to the frictional resistance, q_c, determined from the CPT. Meyerhof (1956), for example, proposed that a relationship of the form $q_c = 4N$ could be used. As can be seen in Figure 2 the suggested relationship does not apply to the loose and poorly graded sand deposit at the Holmen test site. The water table at the site was approximately constant throughout the period of testing and was about 1.5 m below the ground surface.

2.2 Instrumentation of Piles

The four instrumented piles each 8 m long are designated by the letters A, B, C and D. Except for pile C which was conical, the other three piles were cylindrical. Consequently, the positions of the gauges are only presented for pile DA are in Table 1 and Figure 3. A load cell of 75 ton capacity was fixed to the bottom end of each of the piles A and C and was used to measure the point bearing load at any stage, during a test. Vibrating wire gauges were mounted on the reinforcement and embedded in concrete for the measurement of axial load. All the earth pressure cells were mounted on one of the flat surfaces of the pile and were used to record the total pressure. The load cell, the gauges in concrete and in steel, and the earth pressure cells will be described subsequently. The working principle of the vibrating wire gauges and their advantage over the other types of gauges have already been studied in detail in NGI Technical Report No. 9 (NGI, 1962). These instruments are fully described in F.273.0 and will only be briefly described here.

Table 1 Position of gauges in pile DA

Depth, m	Type of Measuring Device	Designation
0.00	External Load Cell	-
1.00	Earth Pressure Cell	1 BL
1.50	Steel Gauge	Gr (71 to 74)
1.65	Concrete Gauge	Re 7
2.50	Earth Pressure Cell	2 BL
3.50	Steel Gauge	Gr (61 to 64)
3.65	Concrete Gauge	Re 6
4.50	Earth Pressure Cell	3 BL
5.50	Steel Gauge	Gr (51 to 54)
5.65	Concrete Gauge	Re 5
6.50	Earth Pressure Cell	4 BL
7.35	Concrete Gauge	Re 4
7.50	Steel Gauge	Gr (41 to 44)
8.50	Earth Pressure Cell	BL 4
9.50	Steel Gauge	Gr (31 to 34)
9.65	Concrete Gauge	3 hvit
10.50	Earth Pressure Cell	BL 3
11.50	Steel Gauge	Gr (21 to 24)
11.65	Concrete Gauge	2 hvit
12.50	Earth Pressure Cell	BL 2
13.50	Steel Gauge	Gr (11 to 14)
13.65	Concrete Gauge	1 hvit
14.50	Earth Pressure Cell	BL 1
16.00	Load Cellar Base	K (22)

2.3 Load Cell at the Base of Pile

The load cell used at the base was water-tight and was the same as that used by DiBiagio and Kjaernsli (1961) for measuring loads under water in strutted excavations. It consisted of a metal cylinder to which is mounted a single vibrating wire gauge and two water-tight end plates. The electric cables come out of the cell through a watertight pot and is connected to a cable leading up to the upper end of the pile. The cell was calibrated before and after the testing programme in a special testing machine. This cell is described in detail in NGI Technical Report No. 9 (NGI, 1962). A schematic drawing of the cell and its calibration are given in Figure 4 a) and b), respectively.

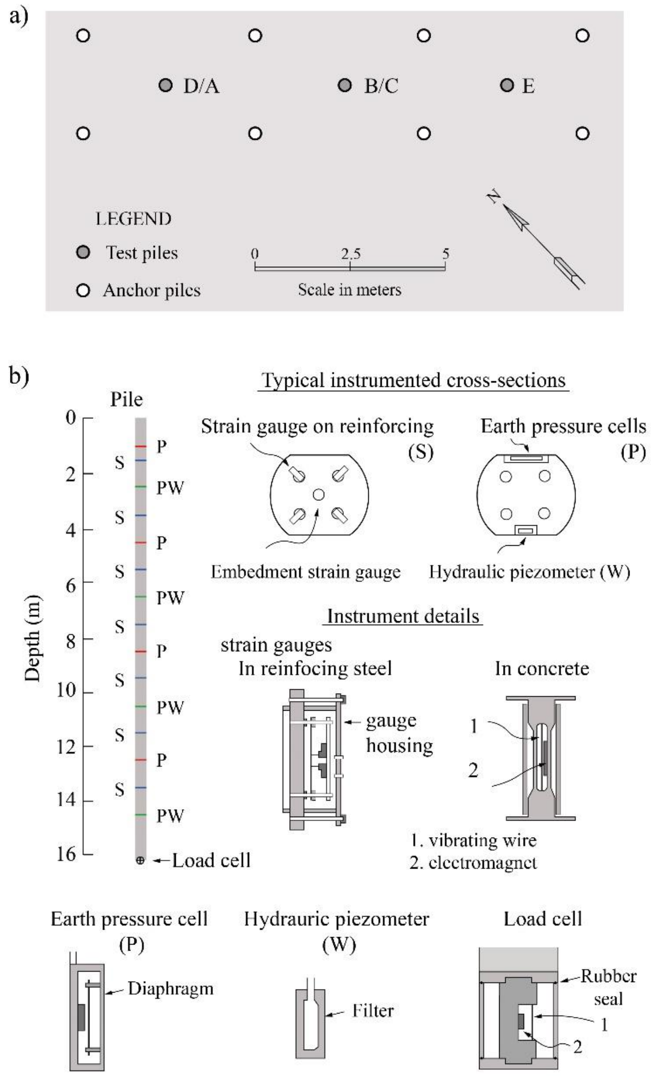

Figure 3 Details of pile test; layout of the test piles and anchor piles (a), instrument details (b) (after Gregersen et al., 1973)

Gregersen et al (1973) concluded that the stability of the load cells used to measure the force at the tip of the piles was quite satisfactory. Measurements taken before pile driving and after recovery of the gauges at the end of the test program indicated a slight change in the zero frequency for the instruments probably as a result of the pile driving. However, this change amounted to only about 1 ton or approximately 1.5 % of the rated capacity of the cell and is therefore not of any great significance.

2.4 Earth Pressure Cell

The earth pressure cells used in the piles were the same as those developed by NGI for measuring earth pressure acting against sheet pile walls. This gauge was described by Øien (1958) and had been subsequently improved. The improved gauge consists essentially of a robust housing which supports by means of three steel balls a diaphragm to which is mounted a vibrating wire strain gauge. The housing is fitted to the flat surface of the pile and is fastened with a screw. Earth pressure acting against the diaphragm of the gauge causes it to deform and thus changes the natural frequency of the vibrating wire. By calibrating each gauge in a pressure tank before use, earth pressures can be determined in the field by measuring changes of vibrating frequency of the wire in the gauge and by using the results of the calibration test. A sketch of the cell and its calibration are shown in Figure 4 c) and d), respectively.

Gregersen et al (1973) was also concerned on the performance of the earth pressure cells: A complete presentation of the data from the earth pressure measurements, is beyond the scope of this paper. In general, the pressure distributions are characterized by a good deal of scatter for all the piles but the measured changes in earth pressure were relatively small throughout the entire test program. This fact is illustrated in Figure 4 e) which shows the range of variation in measured earth pressure during the tests in comparison to the total overburden pressure and pore water pressure.

2.5 Gauge in Concrete

To measure stresses and strains in concrete, NGI developed a gauge which was used for the first time in the piles tested in Holmen. This gauge consists of a split tubular casing surrounding a tube with two end pieces and on which is mounted a vibrating wire gauge. The magnet system of the gauge is kept in position by two counter sunk screws clamped to a small piece of brass. The tube containing the vibrating wire is clamped in position by two cylindrical set screws (See Figure 4 f)).

The following comments by Gregersen et al (1973) on the zero of the strain gauges in all the instrumentation used are worthy of mentioning: "A comparison of the strain gauge zero readings for unloaded piles before driving and after recovery of the piles-indicates that for the majority of the instruments the gauge-wire frequencies increased during the test program. This fact indicates that the tension in the gauge-wire increased and that the gauge-wire was longer than it had been originally. One would expect that if a change in zero frequency were to occur during the test program it would in all probability be a decrease caused by slippage of the wire at the gauge-wire supports. It is felt at this time that the observed increase in zero frequency for the strain gauges are probably associated with the formation of the cracks in the concrete by tensile stress waves in the pile during driving. Expansion of the concrete as it became saturated when driven below the ground water level may also be a contributing factor."

2.6 Gauge in Steel

The stresses and strains in the reinforcement steel were measured by mounting a vibrating wire gauge between two fixed positions as illustrated in Figure 4 h). In this system the vibrating wire is stretched between two steel pins which are previously driven inside the reinforcements bar. The magnet holder is similarly fixed to the reinforcement by two cylinder head screws. The whole arrangement is enclosed in a tube with two end pieces which are made of Perspex. The cables from the gauges are led through one of the end pieces to the cylindrical tube at the centre of the pile and are taken to the surface. At any one section, there are four gauges, mounted one on each of the four reinforcement bars. During calibration, an external load is applied to the pile, the vibrating wire frequencies are measured in each gauge, and the mean value of the change of the square of the frequency Δf^2 is computed for each of the two diagonal pairs. Typical calibration curves for the two diagonal pairs of gauges are the same at any one section. These curves are virtually identical and hence a mean calibration curve is plotted for all the four gauges (see Figure 4 g)) and used for the computation of axial load. The gauges used in the steel and their calibration is shown in Figure 4 h) and i).

3. PILE DRIVING TEST

3.1 Pile Driving Data

The total number of blows required to drive the pile to any specific depth is summarised in a table in (Balasubramaniam et al. (1969) for all the test piles and the anchor piles. The weight of the hammer was 3 Metric ton and the drop 0.25 m. The weight of the top cap of the pile was 350 kg. The results are presented in Figure 5. In this figure, the total number of blows was found to be linearly proportional to the square of the pile length.

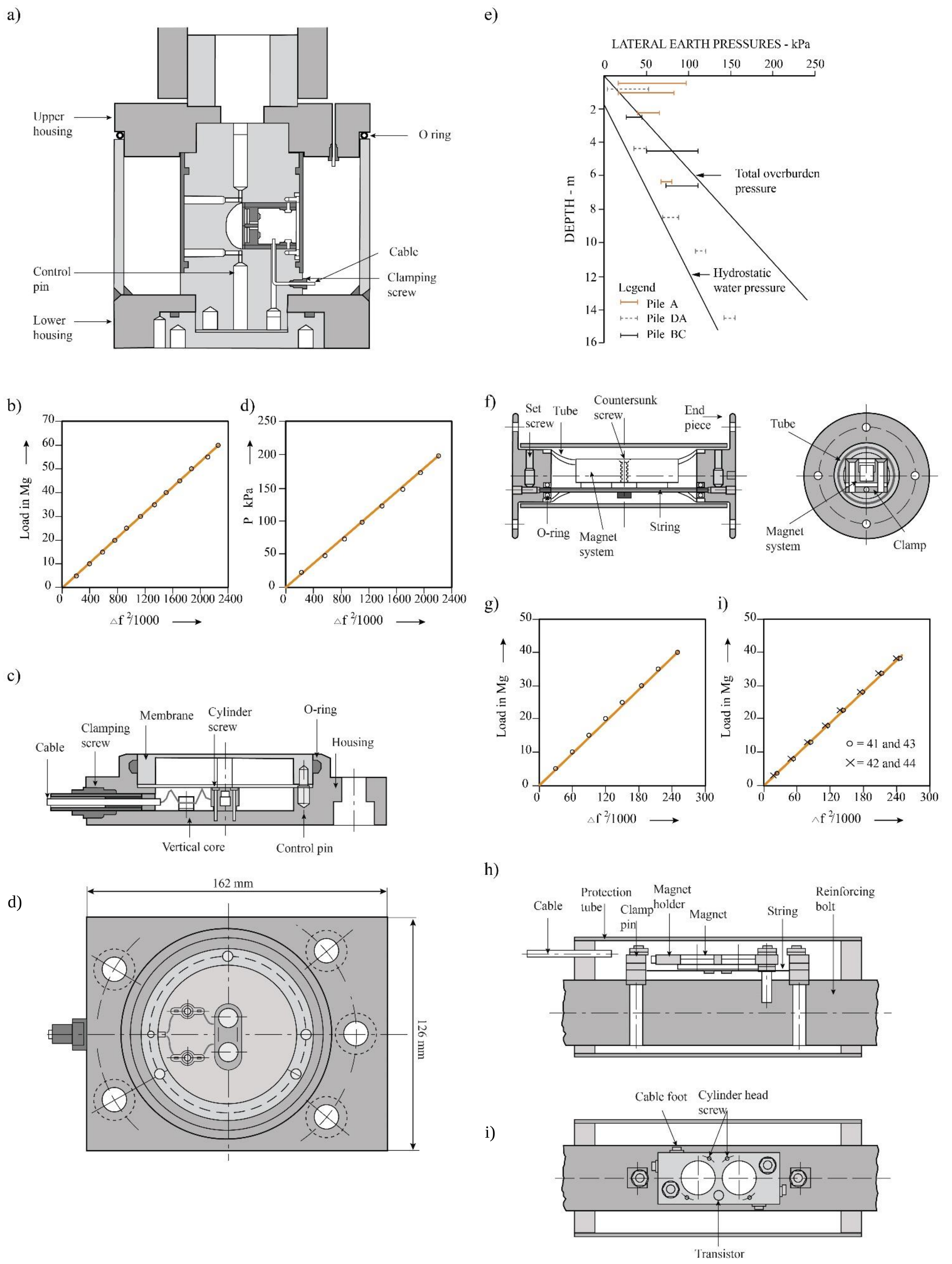

Figure 4 Instrumentation of the piles: Load cell at the base (a), calibration graph for load cell (b), Earth pressure cell (c), calibration graph for the earth pressure cell (d), Variations in measured lateral earth pressure (Gregersen et al., 1973) (e), Gauge in concrete (f), calibration graph for the gauges (conc.) (g), Gauge in steel (h), calibration graph for the gauges (steel) (i)

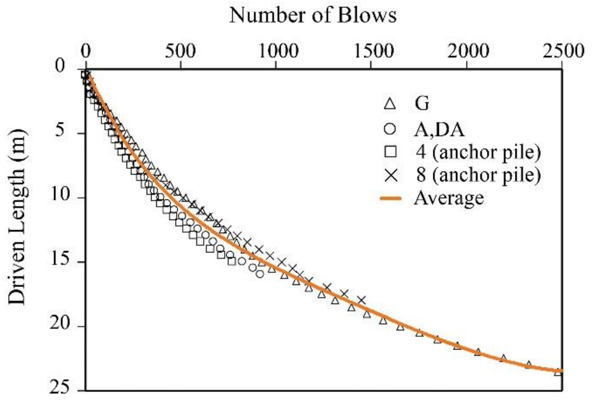

Figure 5 Plots number of blows versus pile penetration

3.2 Pile Testing Procedure and Test Program

The equipment for loading tests consisted of a heavy mild steel joist supported transversely from two others, the latter bolted down to the anchor piles. The load was applied by a hydraulic jack resting on the test pile, obtaining its reaction from the joist above. The applied load was measured by a load cell placed in between the hydraulic jack and the joist. Loads were applied in steps of 3 Metric ton for the 8 m piles and increased proportionally for the piles tested with other lengths. Each increment of load was maintained for 15 minutes. Frequency measurements from all the gauges were taken for each load increment at the end of 1, 5 and 15 minutes. The settlement of the pile was measured on two dial gauges clamped to horizontal bars, one on each side of the pile and resting on horizontal beams fixed to two rigid supports. Settlements were read at intervals of 1, 2, 3, 5, 10 and 15 minutes after the application of each load increment. The overall testing programme is summarised in Table 2.

Altogether 36 tests were carried out on the instrumented piles A, C, DA and BC, and the pile E. A series of 8 tests were conducted on each of the piles A and C which were 8 m long. During test no. 1 in each series, the piles were loaded up to the working load and then unloaded to zero. In test no. 2, the piles were loaded very nearly to the peak load and then unloaded to zero load.

Test no. 3 was continued up to the maximum load and hen unloaded to zero load. During tests no. 4, the piles were again loaded up to the peak value and then unloaded to zero load. Before conducting test no. 5, each pile was driven further by about 50 blows and then tested to the maximum load. In test no. 6, six cycles of working load were applied to each pile and then they were tested to the maximum load again in test no. 7. The series of tests on each pile was completed with test no. 8, which was a pull out test. For the piles DA and BC which were 16 m long, test no. 5 was not conducted and therefore each series of tests for these piles only consisted of the other seven tests.

Six additional tests were conducted on pile E. These tests were performed with driven lengths of 3.5, 7.5, 11.5, 15.5, 19.5 and 23.5 m. A seventh test was conducted on pile E, which was a pull out test on the 23.5 m length piles. All tables related to the tests are given in the test report (Balasubramaniam et al., 1969), meanwhile summarised version of the tables included in this paper.

4. RESULTS

4.1 Load Settlement Characteristics

The load settlement characteristics for all the load tests conducted on the instrumented piles DA and BC are shown in Figure 6. The load settlement characteristics for all the load tests conducted on the instrumented piles A and C were similar to those of DA and BC and are therefore not presented. In Figure 6 the full lines correspond to the tests conducted on the cylindrical pile DA and the dotted line corresponds to the tests on the pile BC.

Table 2 Details of overall testing programme

Date	Pile Desig-nation	Shape of Pile	Length of Pile (m)	Test No.	Remarks
1-7-69	A	Cylindrical	8	1	Load Test
1-7-69	"	"	"	2	"
1-7-69	"	"	"	3	"
2-7-69	"	"	"	4	"
2-7-69	"	"	"	5	"
3-7-69	"	"	"	6	Cyclic Loading Test
3-7-69	"	"	"	7	Load Test
8-7-69	C	Conical	"	1	"
8-7-69	"	"	"	2	"
8-7-69	"	"	"	3	"
9-7-69	"	"	"	4	"
9-7-69	"	"	"	5	"
10-7-69	"	"	"	6	Cyclic Loading Test
10-7-69	"	"	"	7	Load Test
23-7-69	"	"	"	8	Pull out Test
24-7-69	A	Cylindrical	"	8	Pull out Test
18-8-69	DA	"	16	1	Load Test
18-8-69	"	"	"	2	"
18-8-69	"	"	"	3	"
19-8-69	"	"	"	4	"
20-8-69	"	"	"	6	Cyclic Loading Test
20-8-69	"	"	"	7	"
22-8-69	BC	B-Cylindrical	"	1	Load Test
22-8-69	"	C-Conical	"	2	"
22-8-69	"	"	"	3	"
25-8-69	"	"	"	4	"
26-8-69	"	"	"	6	Cyclic Loading Test
26-8-69	"	"	"	7	Load Test
27-8-69	"	"	"	8	Pull out Test
27-8-69	DA	Cylindrical	"	8	"
3-9-69	G	"	3.5	1	Load Test
3-9-69	"	"	7.5	2	"
3-9-69	"	"	11.5	3	"
4-9-69	"	"	15.5	4	"
4-9-69	"	"	19.5	5	"
5-9-69	"	"	23.5	6	"
5-9-69	"	"	23.5	7	Pull out Test

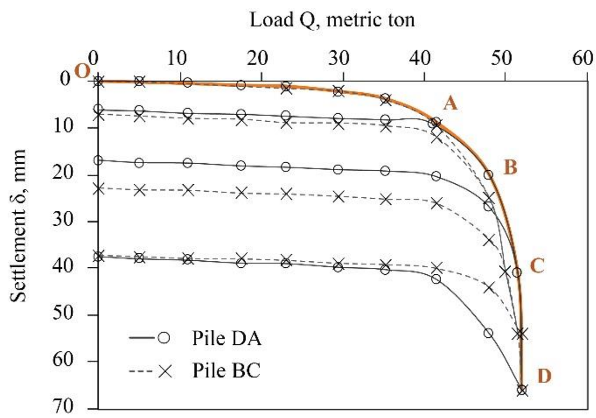

Figure 6 Load cumulative settlement graphs

It is noted that the load settlement curves of all the tests conducted approach an outer envelope as represented by points OABCD (for pile DA). This envelope separates the states of accessible settlements from those which are not accessible. For all states below this boundary the settlement was found to be approximately linear with load and virtually elastic, except for those states which were closer to the envelope. The settlement during cyclic loading at working load was fully recoverable and approached a constant value with increasing number of cycles. This would indicates that for all practical purposes a pile could be cyclically loaded at its working load without appreciable plastic settlement.

The load deformation characteristics of a series of tests on piles of length 3.5 m to 23.5 m (in steps of 4 m) are shown on a cumulative scale in Figures 7 a) and b). These tests were conducted at the same location, and it is clear that there is no unique load-settlement envelope, indicating that the effect of ramming has erased the memory of the previous loading history on the subsequent tests. Figure 7 b) contains the load settlement curves for all the tests conducted on pile E, (with driven lengths varying from 3.5 m to 23.5 m in steps of 4 m) where the loads corresponding to any specific settlement were found to be approximately proportional to the ultimate carrying capacity. The load was therefore normalized for each curve by dividing by the corresponding ultimate bearing capacity, Q_{max}. These results are shown in Figure 8, where the settlement was plotted with respect to the parameter (Q/Q_{max}) relationships for all the tests were found to be the same for a first degree of approximation. So far the analysis has been confined only to total settlement. The total settlement can be separated into two components; (i) a recoverable component and (ii) irrecoverable settlement.

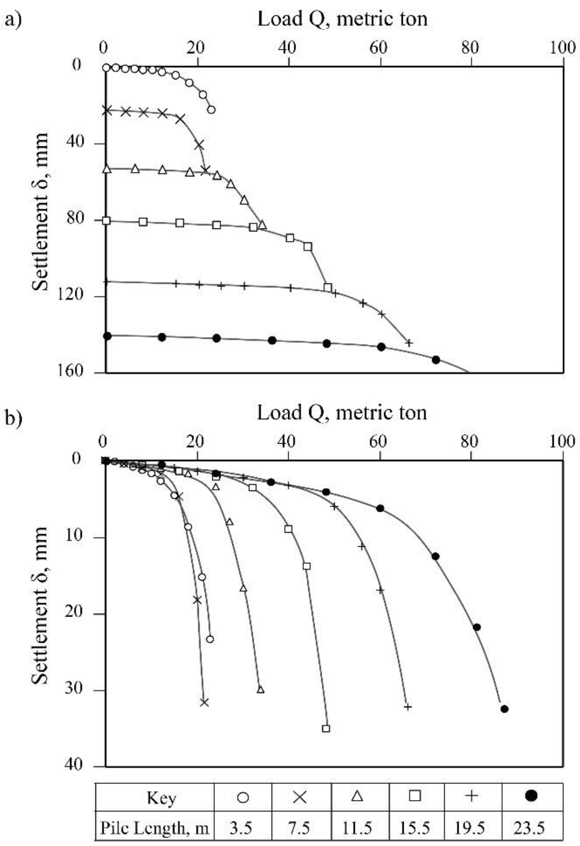

Figure 7 Settlement graphs for pile E (length varied from 3.5 to 23.5m); load-cumulative settlement (a), individual settlement (b)

An assessment of the recoverable settlement, as made from the results of the unloading tests on piles A, C, DA and BC is given in Figures 9 a) and b). In these figures the recoverable settlement was found to be remarkably linear with the applied load.

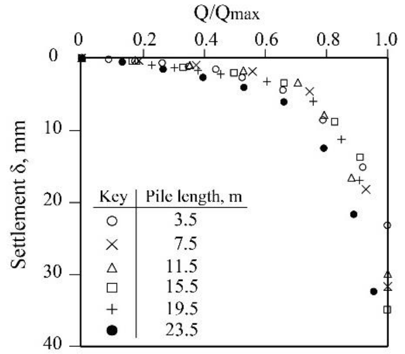

Figure 8 Normalized load-settlement graph for tests in pile E

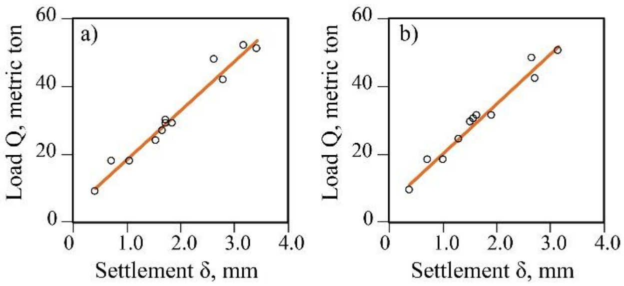

Figure 9 Recoverable settlement: for 8m length pile (a) and 16m length pile (b)

4.2 Lateral Pressure Measurements

For all the tests conducted on the instrumented piles, the total lateral pressure as recorded by all the earth pressure cells was found to be virtually constant up to the working load. However, for further increase in the load, there was a tendency for the lateral pressure to increase in some gauges and to decrease in others, though this variation is small in most cases and can be neglected for all practical purposes. Also, the variation in the lateral pressure was found to be recoverable when the load was removed. This phenomenon could perhaps be explained as being due to either the elastic compression of the pile or its buckling (due to small eccentricities), or possibly to a combination of both (Balasubramaniam et al., 1969).

The effective lateral pressure distributions in the piles were presented in Figure 10 a) at working load (about 18 ton) and at the maximum load (about 52 ton). Although there is no definite order in the distribution of the effective lateral pressure, a clearer picture emerges when the variation of the coefficient of lateral pressure (K) is noted in Figure 10 b).

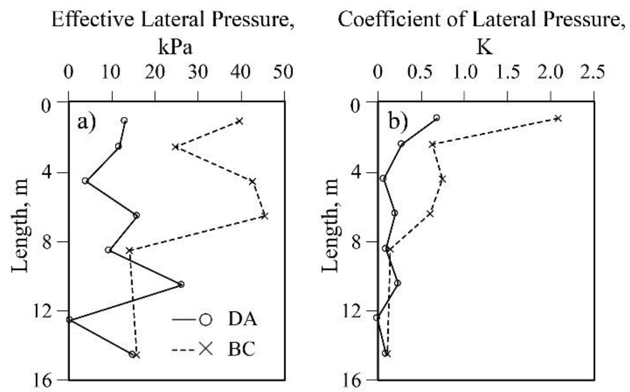

Figure 10 Lateral earth pressure distribution: effective lateral pressure (a), variation in lateral earth pressure coefficient (b)

In these figures the coefficient of lateral pressure is found to decrease from top to bottom in all the piles tested from a value at the top being of the same order as the passive earth pressure coefficient. This observation was independently noted by Mohan et al. (1963), who employed a different technique to those adopted here for the measurement of lateral pressures. Though the possibility remains that the layers of sand close to the surface of the pile will be in a disturbed state, there is no doubt that there is a trend in the distribution of the coefficient of effective lateral pressure K.

4.3 Axial Load Distribution

The measured load is plotted with respect to the applied load as measured by the steel gauges in Figure 11. The variation is remarkably linear. Thus, the load transfer in the piles is also linear. Also, the steel gauges are functioning well. The axial load distribution in piles DA and BC due to external loading are shown in Figures 12 a) and b) at the working load (18 metric ton) and at the maximum load (52 metric ton). In these figures the axial load is found to decrease linearly with depth. The skin friction due to external loading at the maximum load is therefore a constant for the cylindrical pile and decreases linearly with depth for the conical pile.

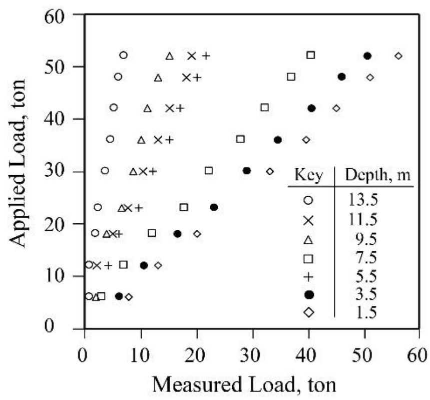

Figure 11 Applied load versus measured load from gauges in steel pile E

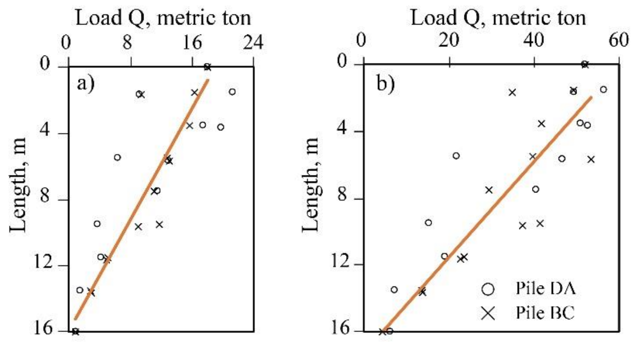

Figure 12 Axial load distributions in pile DA and BC at working load 18 Metric ton (a) and at maximum load (b)

The measured distribution of axial load in the instrumented piles is shown in Figure 13 as demonstrated by Gregerson et al. (1973). The loads at the top and bottom of the piles were determined by the load cells whereas the intermediate values were derived from the strain gauges. At each of the instrumented cross sections of the pile the loads were determined independently from the embedded concrete strain gauge and the gauges attached to the reinforcing steel. These are shown by different symbols in the figure. The distribution of load is shown for three key stages of the test program. Curve I is an estimate of the axial load in the pile measured after the pile had been driven and prior to the first test loading. Curve II is the measured load distribution at an applied load equivalent to one-half of the bearing capacity Q_{90}, and curve III shows the distribution of axial force in the pile at Q_{90} loading. Curve I indicates clearly that there are considerable axial forces in the pile after it had been driven. In the figure, the difference in abscissae between curves I and II or I and III represents the additional increment in load caused by the indicated external test load applied to the top of the pile.

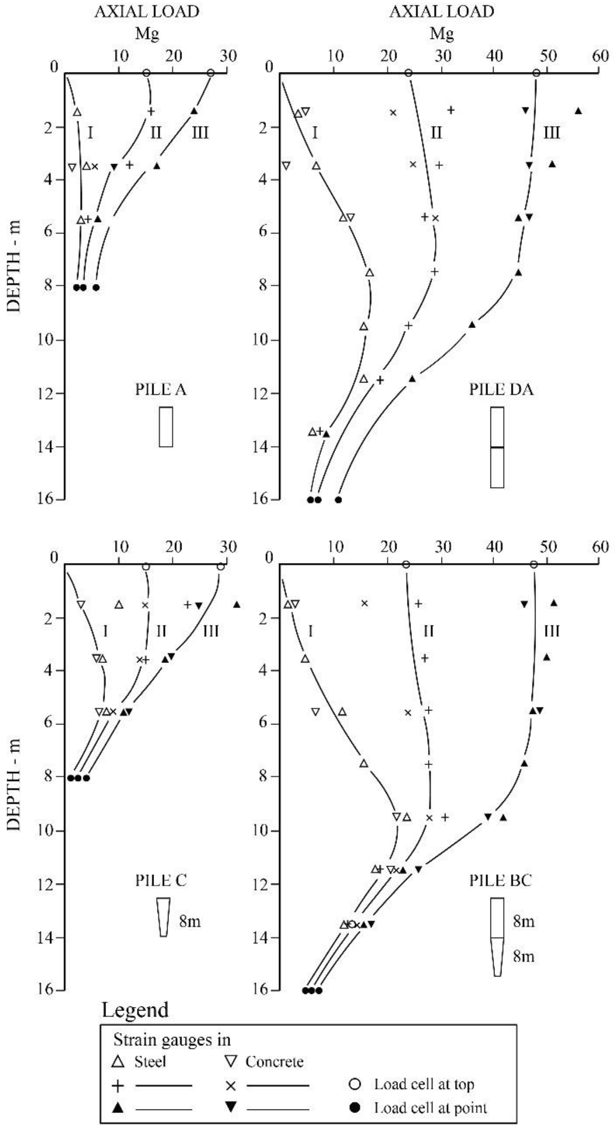

Figure 13 Axial load distribution with depth (after Gregersen et al., 1973)

The load tests also showed that curve I was not representative for the load distribution in the piles at zero external load if the piles had once been subjected to permanent settlements in a loading test. In that case the residual forces were considerably reduced compared to after pile driving. For pile BC this change is illustrated by the difference between curve I in Figure 13 and the curve "After last load test" in Figure 14.

The smooth curves drawn through the data points in Figure 13 have been used to estimate the magnitude of the skin friction developed between the sand and the piles. The skin friction values are shown in Figure 15. Negative values in the figure imply that the sand is hung up on the pile."

As can be seen in Figure 13 significant forces exist in the piles after they are driven. The distribution of this load along the pile followed the same pattern for all piles; it increased down to a point corresponding to about ⅔ of the embedded length and thereafter the force decreased in the lower portion of the pile.

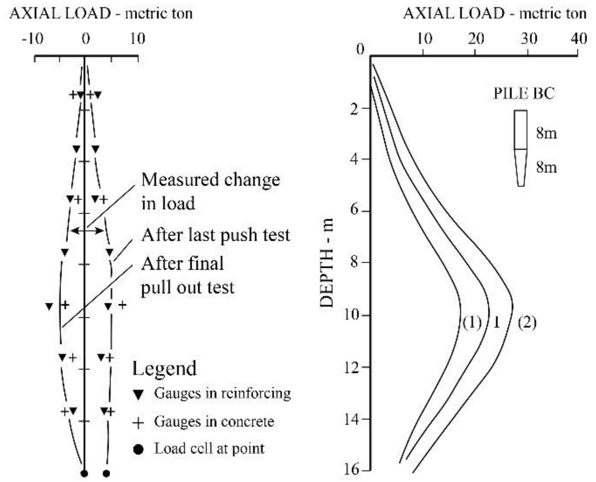

Figure 14 Correction for zero of the gauges due to residual stresses during pile driving (after Gregersen et al., 1973)

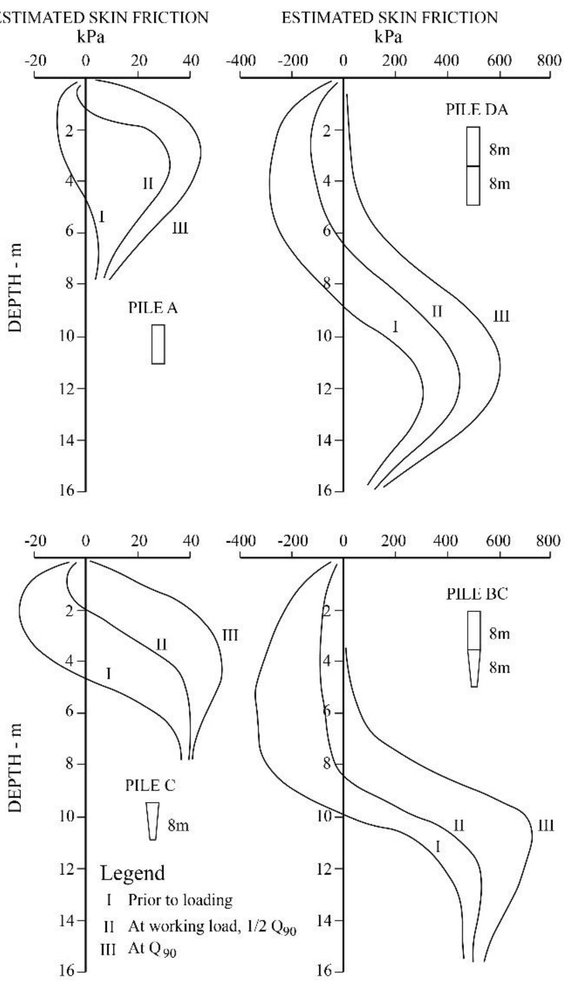

Figure 15 Skin friction values estimated on basis of measured axial loads in instrumented piles (after Gregersen et al., 1973)

In terms of skin friction this implies that frictional forces act in opposite directions along the top and bottom of the pile. These residual forces are somewhat greater for a conical pile than for a cylindrical pile of equivalent length. When the pile is subjected to external loading the frictional forces in the top part of the pile gradually reduce in magnitude and eventually change direction as the load is increased further. For the 8 m long piles this change in direction of the frictional forces occurs at relatively moderate external loads and at Q_{90} there is an upward frictional force acting along the entire length of the pile. For the 16 m long piles, the change in direction of the frictional forces requires a much larger, external load and even at Q_{90} the load transfer to the sand in the top half of the pile is insignificant. For this phenomenon to take place, either the mobilized angle of friction must be small or the earth pressure must be small or a combination of the two. As mentioned previously there was a good deal of scatter in the measured earth pressures for all the piles and the interpretation of these results is therefore somewhat uncertain. However, for the 16 m piles there was a clear tendency for the lateral pressures along the upper half of the piles to reduce once they started penetrating, during application of the external load. A possible explanation for this reduction in pressure may be that, after a sufficient movement between pile and sand, the sand surrounding the pile was subjected to a permanent decrease in volume.

The variation in the measured load, as determined from the measurements in the steel gauges during a test, is presented in Figure 11. In these figures the measured load at each section is found to be linearly dependent on the applied load. Thus, the skin friction is proportional to the applied load. A similar trend is also exhibited by the concrete gauges in Figure 16, that is the measured load at each section being linearly dependent on the applied load. Similar observations were noted for the measurements carried out on piles A and C- 8m long.

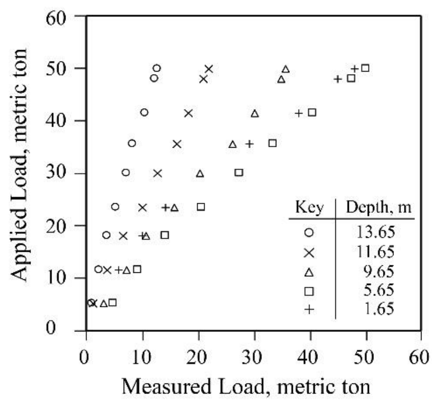

Figure 16 Variation in measured load versus the applied load as indicated by the gauges in concrete

The variation of the point bearing load is presented in Figure 17 for piles DA and BC. The variations are found to be nonlinear in these figures, and the point bearing load is approximately a tenth of the applied load at its maxi mum value. As the applied load is increased, the layer of sand immediately below the point will be compressed and as a result there will be an increase in the point bearing load.

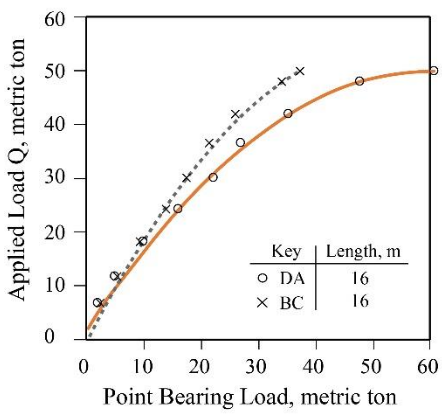

Figure 17 Load transferred to the point as a function of applied load

Finally, the carrying capacity of the piles is the sum of skin friction and end bearing (see Figure 18). Indeed most of the load is carried in skin friction with only a small proportion of the load going to the point at the base.

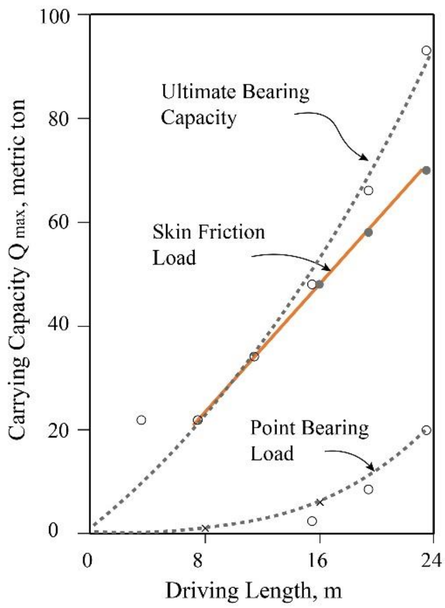

Figure 18 Variation of skin friction, point bearing load and carrying capacity with driven lengths for tests on pile E

The load-settlement curves and the Q_{90} bearing capacity values for the test pile E are shown in Figure 19. for each of the lengths tested. Since the pile was not instrumented only the total applied load is known.

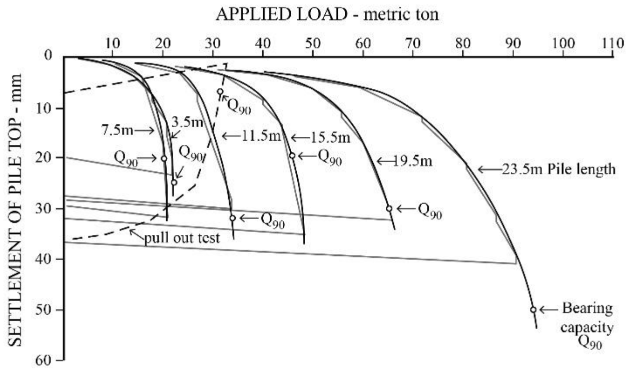

Figure 19 Load settlement graphs for pile E from Gregersen et al. (1973) with pull out test

The load-settlement diagrams for the four instrumented piles in Figure 20 indicate that for the two pile lengths tested there is no significant difference between the bearing capacity of a conical pile and a cylindrical pile; however, the magnitude of the point load and the skin friction do vary somewhat for the two types of piles. The bearing capacity values, Q_{90}, and the corresponding values of the point load as well as the component of load due to skin friction are summarized in Table 3 for each of the instrumented piles. As can be seen from the table the portion of the bearing capacity expressed in percent attributed to the point load and skin friction is fairly independent of the pile length. The ratio of skin friction to point load does differ, however, for a cylindrical pile and a conical pile. In the case of the cylindrical pile the point load accounts for nearly 25 % of the total load whereas for the conical pile the point load is less than 15 % of the applied load. Although the point load is smaller for the conical pile, this reduction in load is equivalent to the reduction in cross sectional area of the tip of the conical pile relative to the cylindrical pile. Consequently, the point resistance or force per unit area is the same for both piles.

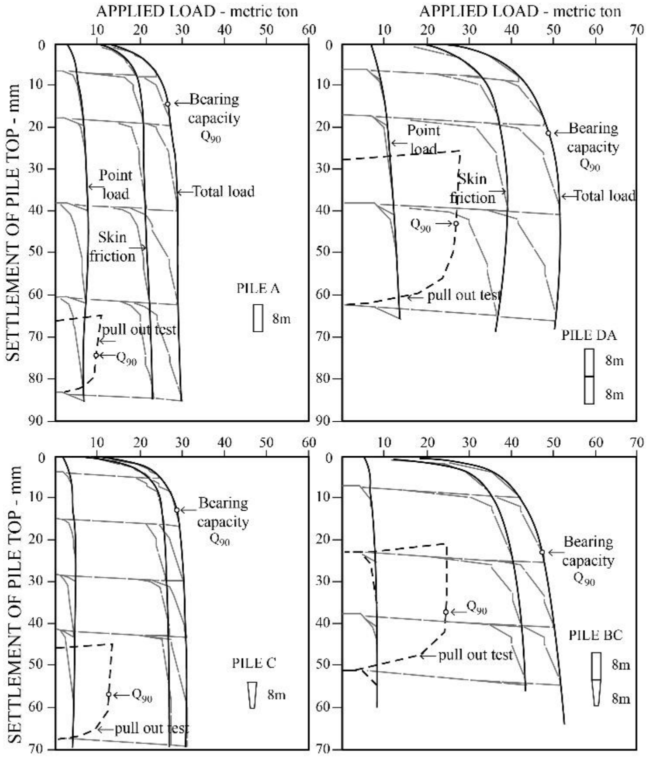

Figure 20 Load settlement graphs of instrumented piles from Gregersen et al. (1973) including pull out tests

Table 3 Point bearing load and skin friction load (at Q_{90} point load) from instrumented piles: after Gregersen et al. (1973)

Pile	Bearing Capacity Q_{90}- metric ton	Point load		Designation	
		metric ton	% of Q_{90}	metric ton	% of Q_{90}
A	27.0	6.0	22	21.0	78
C	28.0	3.5	13	24.5	87
DA	49.0	11.0	22	38.0	78
BC	48.0	7.5	16	40.5	84

The settlement of the piles at the Q_{90} loading amounted to 15 mm and 13 mm respectively for the 8 m long cylindrical and conical test piles while the settlement for the 16 m long piles was 21 mm for pile AD and 23 mm for pile BC. Figure 20 also shows quite conclusively that when the piles are subjected to external tensile loading the bearing capacity is much smaller than when the piles are loaded in compression. A comparison of the skin friction mobilized at Q_{90} for load and pull out tests is given in Table 4. The observed reduction in bearing capacity varyies from 50 to 65 % and the largest reductions are noted with the 8 m long piles.

Table 4 Values of mobilized skin friction for push-and pull-out tests at Q_{90} loading (after Gregersen et al., 1973)

Pile	Skin friction, kPa	
	Load test	Pull out test
A	30	14
C	41	20
DA	27	19
BC	31	19

Since pile E did not have a load cell at its tip, it is not possible to determine directly how much of the load was carried by the point and how much can be attributed to skin friction. However, by comparing the point resistance q_c determined from CPT and the point resistance q_p measured with the four instrumented piles as shown in Figure 21, it appears that the two resistance values can be related by the following approximate expression: $q_p = 1/2\ q_c$. If it is assumed that this relationship is valid for each length of pile E that was tested, then it is possible to make an estimate of the point loads for pile E. These estimated point loads and the corresponding bearing capacity values are shown in Figure 21 for pile E. Within the zone of loose sand where CPT tests indicated a penetration resistance that increased approximately linearly with depth, i.e. from 6 to 8 m in depth, the bearing capacity increases linearly with pile length. Table 5 gives the numerical values of bearing capacity and skin friction for the pile lengths tested. This data shows a moderate increase in skin friction with depth.

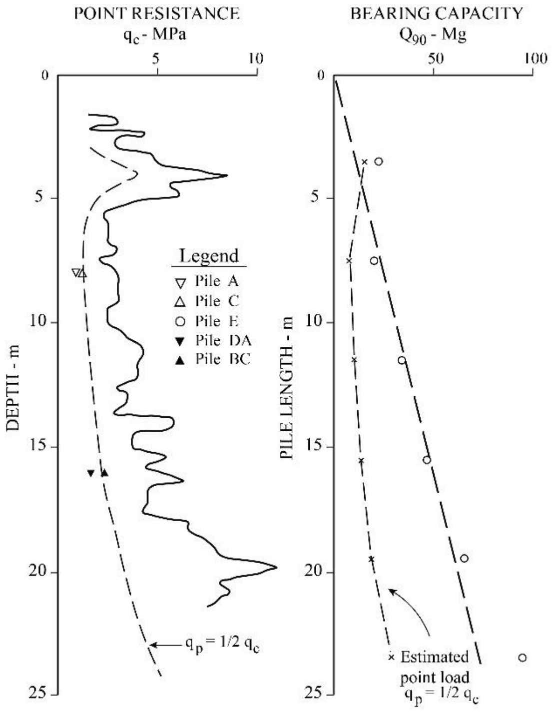

Figure 21 Left: Comparison of CPT and measured point resistance values for the instrumented piles. Right: Measured bearing capacities and estimated point loads for pile E as function of embedded pile length. (after Gregersen et al., 1973)

Table 5 Bearing capacity values and mobilized skin friction for pile E at Q_{90} loading

Properties	values				
Embedment length, m	3.5	7.5	11.5	15.5	23.5
Bearing capacity, Q_{90}, metric ton	22	20	34	46	94
Average calc. skin friction, kPa	22	19	24	24	30

5. CONCLUDING REMARKS

An instrumented pile testing programme carried out in Holmen, Drammen, was interpreted in two different manners. One is NGI Internal Report No. F.273.0 performed by Balasubramaniam et al. (1969). In this interpretation, the zero of the vibrating wire gauges was used as monitored after pile driving and only the load tests were considered. Secondly, Gregersen et al. (1973) interpreted the instrumentation data from the gauge readings before pile driving and also included pull out tests. The interpretation of Gregersen et al. (1973) gave greater insight into the effect of the residual stresses developed during the pile driving and their effect on the interpretation which was not included in NGI Internal Report F.273.0.

The major conclusions can be summarised as following: (1) There exists a unique load-settlement envelope corresponding to any particular length of pile, which separates the states of accessible settlement form those which are not accessible; (2) At any particular loading the settlement observed in a conical pile is found to be smaller than that for a cylindrical pile; (3) The effect of ramming of the pile is found to be negligible on the unique load settlement envelope stated under finding 1, for a limited number of blows (about 22 blows which correspond to a settlement of 20 cm); (4) All settlements observed during cyclic loading at the working load are found to be recoverable and is an order smaller than the settlement corresponding to the maximum load; (5) The recoverable settlement is found to be linearly dependent on the load; (6) A unique relationship exists between Q/Q_{max} and settlement δ where corresponds to the plastic settlement of the pile; (7) The effective lateral pressure is found to be maximum near the top of the pile and is found to decrease with depth towards the bottom end; (8) The value of K, the ratio of the effective lateral pressure to the effective overburden pressure, is found to decrease with depth for all loads up to the maximum load. The minimum value at the bottom varies from 0.1 to 0.4 and is of the same order as the active earth pressure coefficient; (9) The overall pattern in the variations of the effective lateral pressure and K is generally the same for load and pull tests carried out both on cylindrical and conical piles of 8 and 16 m length; (10) The skin friction at any particular load is a linear function of the applied load, i.e. $\tau = (Q/Q_{max})\ \tau_{max}$, where τ_{max} is the maximum skin friction corresponding to the ultimate bearing capacity. (11) The bearing capacity is found to consist of two parts; one being due to skin friction and is proportional to the length of the pile, while the other due to point bearing load and is a non-linear function of the length of the pile; (12) The effect of the residual stress decreased once the piles were load tested. The skin friction in the load tests and pull tests are different as tabulated in Table 4; (13) Bearing capacity values and mobilized skin friction for pile E, at Q_{90} loading are contained in Table 5.

6. ACKNOWLEDGEMENTS

The author is deeply indebted to Dr. Elmo DiBiagio and Mr. Gunnar Aas and for their valuable help and assistance in engaging the first author to work at NGI on this project. This paper is a revised version of the earlier paper published by the first author with the kind permission of the Director, Norwegian Geotechnical Institute. It cements the earlier work presented in the NGI report F.273.0 (Balasubramaniam et al., 1969) and the subsequent paper of Gregersen et al. (1973). Thanks are also due to the Royal Norwegian Council for Scientific and Industrial Research in granting the author a Post Doctorate Research Fellowship to enable him to work at NGI. The authors are really indebted to the hard work and help of Khun Boonjira (Ta) in the editorial works of this paper. Also grateful acknowledgement to Dr E C,Leong, Prof Der Wen Chang, Dr Jayantha Ameratunga, Mr Kyoshi Yamashita, Dr P. Russo, and many others for their helpful comments in improving the quality of the material contained here.

7. REFERENCES

Balasubramaniam, A. S., Dibiagio, E. and Aas, G. (1969) A brief summary of the instrumentation used and the results obtained from instrumented piles tested in sand at Holmen, Drammen. NGI Internal Report No. F.273.0.

Bjerrum, L., T. C. Kenney and B. Kjaernsli, (1965) "Measuring instruments for strutted excavations", Proceedings of American Society of Civil Engineers, Vol. 91, SM 1, pp111-141.

DiBiagio, E. and B. Kjaernsli, (1961) "Strut loads and related measurements on contract 63 a of the Oslo subway", Proceedings of the 5th Int. Conf. on Soil Mech. and Found. Eng., Vol. 2, pp395-401.

Fellenius, B. H, (1975) "Test loading of piles and new proof testing procedure", Journal of the Geotechnical Engineering Division, GT9, pp16-30.

Gregersen, O. S., Aas, G. and Dibiagio, E. (1973) "Load tests on friction piles in loose sand". Proceedings of the 8th Int. Conf. on Soil Mech. and Found. Eng., Moscow, Vol. 3, pp109-117.

Meyerhof, G. G. (1956) "Penetration tests and bearing capacity of cohesionless soils", Proceedings of American Society of Civil Engineers, Vol. 82, SM 1, Paper 866, p18.

Mohan, D., Jain, G. S. and Kumar, V. (1963) "Load bearing capacity of piles". Geotechnique, VI, XIII, no. 1, pp76-86.

Norwegian Geotechnical Institute (NGI). (1962) Vibrating wire measuring devices used at strutted excavations. Technical Report No. 9., p155

Oien, K. (1958) "An earth pressure cell for use on sheet piles". Proceedings of the Brussels Conference on Earth Pressure Problems, Vol. 2, pp118-126.